Strontium-86 labeling experiments show spatially heterogeneous skeletal formation in the scleractinian coral *Porites porites*

Fanny Houlbrèque,[1,2] Anders Meibom,[3] Jean-Pierre Cuif,[4] Jaroslaw Stolarski,[5] Yves Marrocchi,[3] Christine Ferrier-Pagès,[6] Isabelle Domart-Coulon,[7] and Robert B. Dunbar[1]

Received 24 November 2008; revised 8 December 2008; accepted 14 January 2009; published 19 February 2009.

[1] This paper presents the results of an effort to label calcium carbonates formed by marine organisms with stable isotopes to obtain information about the biomineralization processes. The growing skeleton of the scleractinian coral *Porites porites* was labeled three times with enhanced abundances of ^{86}Sr. The distribution of ^{86}Sr in the skeleton was imaged with the NanoSIMS ion microprobe with a spatial resolution of ~200 nm and combined with images of the skeletal ultra-structure. Importantly, the distribution of the ^{86}Sr label in the *P. porites* skeleton was found to be strongly heterogeneous. This constrains the physical dimensions of the hypothetical Extracellular Calcifying Fluid (ECF) reservoir at the surface of the growing skeleton, which is implicit in most geochemical models for coral biomineralization. These new experimental capabilities allow for a much more detailed view of the growth dynamics for a wide range of marine organisms that biomineralize carbonate structures. **Citation:** Houlbrèque, F., A. Meibom, J.-P. Cuif, J. Stolarski, Y. Marrocchi, C. Ferrier-Pagès, I. Domart-Coulon, and R. B. Dunbar (2009), Strontium-86 labeling experiments show spatially heterogeneous skeletal formation in the scleractinian coral *Porites porites*, *Geophys. Res. Lett.*, *36*, L04604, doi:10.1029/2008GL036782.

1. Introduction

[2] Coral-based sea-surface temperature reconstructions are extrapolations of an empirical relationship between skeletal composition (e.g., δ^{18}O or Sr/Ca) and measured sea-surface temperature, resting on the assumption that biological effects (so-called 'vital effects') in the biomineralization process, which might introduce compositional variations unrelated to temperature, are either minimal or constant. However, micro-analytical studies have demonstrated that all coral skeletons are characterized by substantial compositional variation, which is directly related to the skeletal ultra-structure and much too large to be explained by anything but biological activity [*Adkins et al.*, 2003; *Allison*, 1996; *Allison and Finch*, 2007; *Blamart et al.*, 2007; *Cohen et al.*, 2001; *Cuif and Dauphin*, 1998; *Cuif et al.*, 2003; *Meibom et al.*, 2003, 2004, 2006, 2007, 2008; *Nothdurft and Webb*, 2007; *Rollion-Bard et al.*, 2003a, 2003b; *Shirai et al.*, 2005; *Sinclair et al.*, 2006; *Sinclair*, 2005; *Stolarski*, 2003]. These findings complicate the use of scleractinian corals as proxies for paleo-environmental change and raise important questions about the dynamics of the skeletal formation process as well as the biological origin of the compositional variations. Efforts to answer these questions would be greatly aided by a method to precisely label the skeleton under normal growth conditions. Ideally, this marker should be a natural skeletal component and resolvable in the skeleton with a spatial resolution comparable to the micrometer length scales that characterize the skeletal ultra-structure. Such a labeling capability would provide a more detailed understanding of the growth-dynamics and help constrain models for variations in skeletal composition. The objective of the present study is to present a method of labeling the skeleton with the stable isotope ^{86}Sr, with subsequent NanoSIMS ion microprobe imaging and detection of the label in the skeleton. We have carried out experiments with the scleractinian genus *Porites* that is most frequently used for sea-surface temperature reconstructions [*Cole et al.*, 2000; *Fairbanks and Evans*, 1997; *McCulloch et al.*, 1999]. The results reveal important aspects of the growth dynamics with implications for the understanding of the coral biomineralization process.

2. Materials and Methods

[3] Growth experiments were conducted in the laboratory of the Centre Scientifique in Monaco using colonies of the branching zooxanthellate scleractinian *Porites porites*, which is commonly found in coral reefs of the west Atlantic Ocean and along the African coast [*Veron*, 2000]. The colonies used in the experiment were collected from the reef of Guadeloupe Island in the Caribbean Sea (CITES permit FR 04-97100162E), transported to Monaco and maintained for three months in an open-flow aquarium before experiments began. Three micro-colonies were prepared before the beginning of the labeling experiment by cutting terminal portions of branches (~2 cm long and ~1 cm wide) from a parent colony and gluing these fragments onto glass slides, using underwater epoxy (Devcon®) [*Reynaud-Vaganay et al.*, 1999]. These branch tips were maintained in an aquarium supplied with Mediterranean seawater pumped from a depth of 50 m. Throughout the experiment, the water temperature was kept at 26°C, which is optimal for skeletal

[1]Geological and Environmental Sciences, Stanford University, Stanford, California, USA.
[2]Marine Environment Laboratories, International Atomic Energy Agency, Principality of Monaco, Monaco.
[3]Laboratoire de Minéralogie et Cosmochimie du Muséum (LMCM), UMS NanoAnalyses 2679, Muséum National D'Histoire Naturelle, Paris, France.
[4]UMR8148, IDES, Université Paris XI, Orsay, France.
[5]Instytut Paleobiologii PAN, Warszawa, Poland.
[6]Centre Scientifique de Monaco, Principality of Monaco, Monaco.
[7]Département Milieux et Peuplements Aquatiques, UMR5178, Muséum National d'Histoire Naturelle, Paris, France.

0094-8276/09/2008GL036782$05.00

growth. Philips metal halide lamps (HPIT, 400 W) provided an irradiance of 300 μmol photons m^{-2} s^{-1} on a 12h light/12 h darkness schedule. After three weeks of growth, the tissue entirely covered the three micro-colonies and had expanded onto the glass slide. The micro-colonies were then ready to be used for the labeling experiment.

[4] Labeling experiments. The three micro-colonies of *P. porites* were incubated in seawater enriched in $^{86}Sr^{2+}$. Seawater was labeled by adding ~17 mg/l of ^{86}Sr-carbonate powder with an estimated grain-size of about 10–100 μm and an ^{86}Sr isotopic abundance of 97% (commercially available from the Oak Ridge National Laboratory, USA). The resulting increase in the abundance of $^{86}Sr^{2+}$ in the labeled seawater can be inferred from ^{86}Sr concentration increase in the coral skeleton and is discussed below. During labeling, each micro-colony was incubated in 200 ml beakers and the labeled seawater was continuously stirred using small stirring bars and renewed at a flow rate of 4 ml/hour controlled by a peristaltic pump. In each labeling event, the micro-colonies were incubated from 10 AM on one day to 10 AM two days later, i.e., for a total of 72 hours, corresponding to three light/dark cycles. After this incubation the micro-colonies were returned to normal conditions in their aquarium with a permanent renewal of seawater and natural isotopic abundances of Sr^{2+}. After 6 days, the labeling procedure was repeated. In total, three such labeling events were carried out. Throughout the experiment the coral polyps had continuously expanded tentacles during daytime (Figure 1a), indicating unperturbed viability and suggesting that the organism did not suffer substantial levels of stress. At the end of the third and last labeling event, the colonies were returned to normal aquarium conditions for one week before the experiment was terminated and the tissue was removed by the water-pick method. Segments were cut from each micro-colony using a diamond-coated blade and a Buhler saw. These samples were mounted in epoxy, polished down to a 0.25 μm finish with diamond suspensions, gold-coated and imaged with the NanoSIMS ion microprobe at the Muséum National d'Histoire Naturelle in Paris.

[5] NanoSIMS analyses were carried out with a primary beam of negatively charged oxygen focused to a spot-size of ~200 nm on the surface of the sample. The secondary ions $^{44}Ca^{+}$ and $^{86}Sr^{+}$ were detected in multi-collector mode with electron multipliers at a mass resolving power of ~5000, which allows all potentially problematic mass-interferences to be resolved [*Meibom et al.*, 2004, 2008]. Images of 256 by 256 pixels were obtained by rastering the primary beam across a pre-sputtered surface with a pixel dwelling time of 10 ms. Following NanoSIMS imaging, the coating was removed and the samples lightly etched by ~1 % formic acid. This brings out the ultra-structural details of the skeleton. The samples were then recoated with gold and observed in a Phillips XL30 scanning electron microscope (SEM). Additionally, entire fragments of micro-colonies were etched with formic acid, coated with carbon and gold and imaged with a TESCAN (Vega II LSU) SEM.

3. Results and Discussion

[6] Several different types of markers have been used to study and date coral skeletal formation. Alizarin red and calcein, for example, are frequently used to stain different stages in growth formation on time scales of weeks to years. The alizarin stain in the skeleton is visible to the naked eye, whereas the calcein fluorochrome bound to the skeleton is induced to fluoresce by filtered light (excitation filter BP450-490 nm, emission filter LP515 nm). Such stains are therefore easily identified along growth fronts. As such they provide useful time markers from which skeletal growth rates can be deduced. However, the use of dye markers is problematic when the goal is to understand more specific aspects of the skeletal formation processes. The physiological response of coral polyps to the exposure of chemical dyes is not understood in detail, but it is generally accepted that alizarin may be toxic and can have a negative short-term impact on coral calcification. For example, a hermatypic coral, *Diploria strigosa*, exposed to alizarin for 24 hours was observed to decrease its calcification rate for a period up to 6 days after the labeling event [*Dodge et al.*, 1984]. Calcein has a high affinity for divalent cation Ca^{2+}

Figure 1. (a) A micro-colony (~2 cm in vertical dimension) of *Porites porites* with fully expanded polyps photographed during labeling with ^{86}Sr enriched seawater. (b) SE micrograph of the skeleton surface of a fragment of a microcolony after tissue removal. Five complete corallites with polygonal boundaries are visible. The contour of one corallite is outlined. (c) Enlargement of corallite showing porous (reticulate) septa (marked with arrows) and their vertical projections. (SE micrograph.) (d) Granulated (tuberculate) texture (black arrow) of the surface of a vertical projection from septa. (SE micrograph.) (e) Concentric layers of aragonite fibers surrounding a calcification center (white arrow) and granulated texture of the outer surface (black arrow) in broken and etched section of vertical calicular projection. (SE micrograph.) (f) Reflected micrograph of a polished and Au-coated section of micro-colony indicating some of the regions imaged with the NanoSIMS. (g–i) NanoSIMS images of the ^{86}Sr distribution in labeled skeleton. Blue regions indicate normal (i.e., unlabeled) $^{86}Sr/^{44}Ca$ ratios. Red-yellow regions indicate enhanced $^{86}Sr/^{44}Ca$ ratios due to the labeling. (g) Cross-section of a vertical projection from septa (c.f. Figure 1f) clearly showing all three labeling events as concentrically expanding growth fronts. Inset shows a NanoSIMS line-scan along the hatched line in Figure 1g across three ^{86}Sr labels. During each labeling event the $^{86}Sr/^{44}Ca$ ratio of the skeleton increases by about a factor of 4–6. (h) Skeletal region showing the last two ^{86}Sr labeling events. The ^{86}Sr label is not continuously distributed along the growth front, but forms clearly separated hotspots. Occasionally the hotspots may be linked to form sausage-chain structures. (i) NanoSIMS image showing ^{86}Sr-labeled hotspots from the last labeling event superimposed on SE micrograph of the lightly etched surface of the skeleton exhibiting the fibrous ultra-structure. Note that the last labeled ^{86}Sr hotspot in some places intersect the surface of the skeleton (Figures 1g and 1i), most likely due to removal of a few micrometers of the outermost skeleton during preparation. See text for discussion.

and a low affinity for Mg^{2+} [*Chiu and Haynes*, 1977] and may alter some cell functions and thus potentially perturb the coral biomineralization process, as shown in several marine mollusk experiments in which calcein was observed to decrease shell increments [*Thébault et al.*, 2006]. A coral stained with alizarin or calcein obviously recovers from this stress and continues to grow. But if, as it is the case here, the objective is to study micron-scale details of the biomineralization process while the skeleton is being labeled, any stress on the organism inflicted by the labeling agent during exposure might invalidate the observations. The labeling experiments presented here offer an alternative to the addition of chemicals to the seawater.

[7] Examples of the data obtained by the new technique are shown in Figure 1, which summarizes the skeletal ultrastructure and the distribution of the ^{86}Sr label in the skeleton as a result of the labeling experiments.

[8] All three labeling events were clearly observed in the skeleton (Figure 1). During each labeling event, the ^{86}Sr concentration of the skeleton increased by a factor of about 4 to 6 compared to the unlabeled skeleton (Figure 1g, inset). Strontium and Ca are, to first order, incorporated into the skeleton in proportion similar to their elemental ratio in seawater and fractionation between different Sr isotopes is insignificant [*Fietzke and Eisenhauer*, 2006]. Therefore, the labeled seawater was enriched in $^{86}Sr^{2+}$ by a factor similar

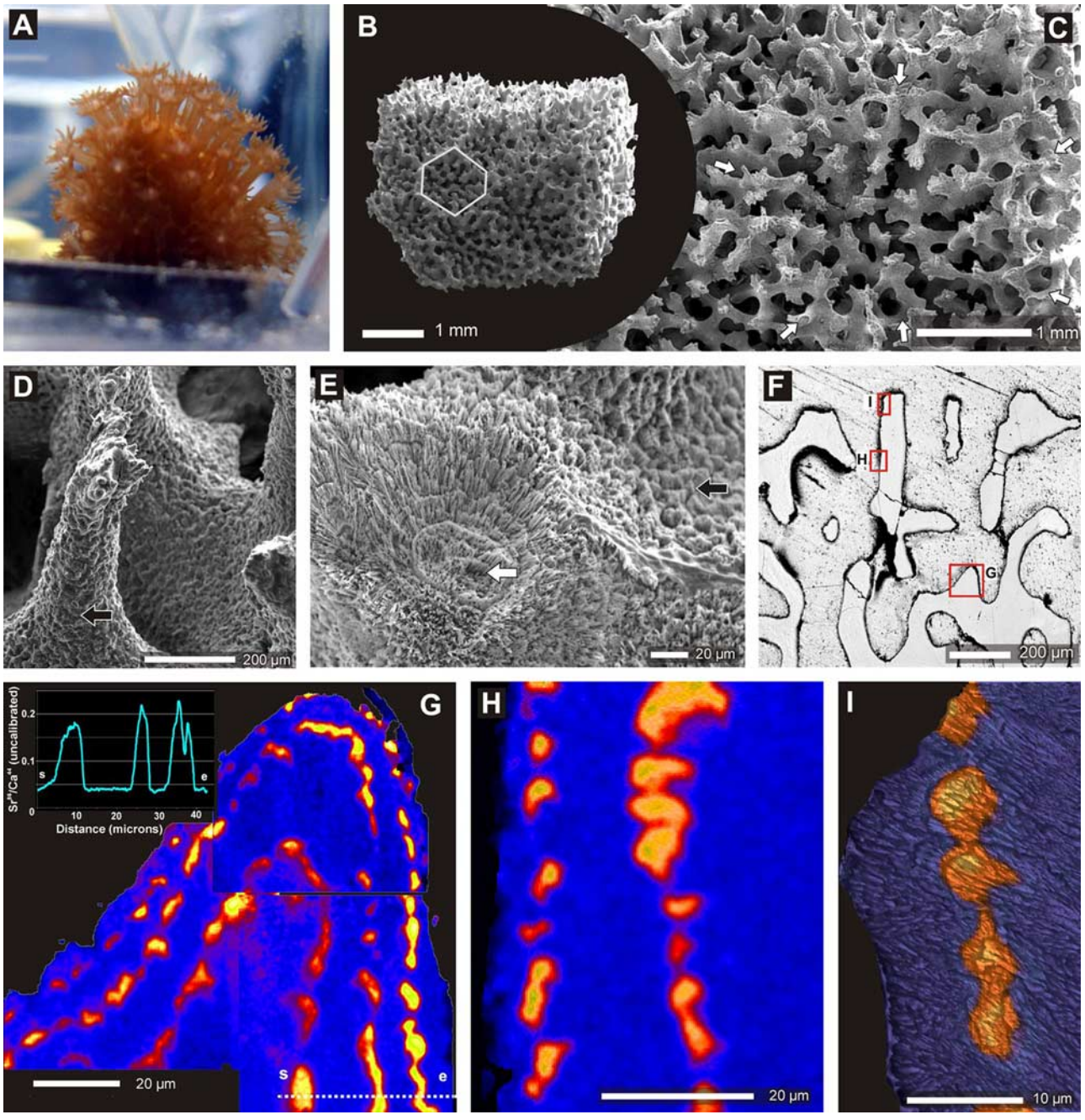

Figure 1

to the enrichment observed in the skeleton. An increase in the $^{86}Sr^{2+}$ concentration by a factor of 4 to 6 in the labeled seawater corresponds to an increase in the total Sr^{2+} concentration of about 50%. This is likely to have a minimal impact on the physiological processes of the coral. The Sr^{2+} ion is, together with Ca^{2+} transported by the Ca-ATPase enzyme [*Ferrier-Pagès et al.*, 2002] and the Sr/Ca ratio in the skeleton is on the order of 10 mmol/mol, similar to their ratio in seawater. This means that, under normal (i.e., unlabeled) conditions, on average 1 Sr^{2+} ion is transported to the skeleton for every 100 Ca^{2+} ions. Under the labeled conditions in this study, this ratio was changed to 1.5 Sr^{2+} ions per 100 Ca^{2+} ions, which seems unlikely to have a large perturbing effect on the biomineralization processes. Nevertheless, future studies will be aimed at defining the minimum abundance of $^{86}Sr^{2+}$ in the labeled seawater and the minimum labeling time-scale that enable unambiguous detection of the label in the skeleton with the NanoSIMS, while carefully monitoring possible effects on skeletal growth-rate and metabolism, including expression of coral stress proteins.

[9] It is clear that the experiment demonstrates the potential of stable isotopic labeling to accurately identify the site of carbonate deposition and that stable isotopic labeling techniques open up a large number of interesting applications in the study of biomineralization by marine carbonate producing organisms. In the following we discuss some interesting observations that demonstrate the potential of the technique and/or have immediate implications for understanding of coral biomineralization.

[10] First, the skeletal growth rate between the three labeling events seems to differ significantly. Judging from Figure 1g, on average the coral seems to have added more to the skeleton in the week between the first and the second labeling than between subsequent labeling events. But, at the same time, the growth rate also differs markedly between different directions in the skeleton. Along the vertical growth axis in Figure 1g, the growth rate was more than 20 μm between the first two labeling events, whereas perpendicular to the axis, the growth rate was less than half. In future experiments with even shorter labeling time-scales, this type of observation will yield a very detailed picture of the growth dynamics of any coral species, provided that it can be maintained under conditions that allow substantial skeletal formation to take place.

[11] Second, even taking into account the large observed variation, the skeletal growth rates in the aquarium seem relatively low compared to those of *Porites sp*. living in nature. There, *Porites sp.* can easily form skeleton at rates up to 21 mm per year, which is equivalent to 58 μm per day (vertical extension rate) [*Huston*, 1985]. However, in general the micro-colonies seemed to be healthy (continuously expanded tentacles during daytime) and the growth rates observed in our experiments are not significantly different from that of other *Porites porites* living in aquariums under similar conditions [*Marubini*, 1996]. This leads us to believe that the labeling experiments have not affected the growth rate of the micro-colonies. Still, natural conditions do seem to favor higher growth rates. An important objective for future studies will therefore be to label corals growing with high growth rates under natural conditions.

[12] Third, as illustrated in Figure 1i, it is possible to combine NanoSIMS images showing the distribution of the isotopic label in direct relation with the skeletal ultrastructure imaged with an SEM. For short labeling time-scales, this type of combined imaging opens up the possibility to determine the exact order in which different ultra-structural components (i.e., centers of rapid accretion/early mineralization zone and fibrous skeleton) form [*Cuif and Dauphin*, 2005; *Stolarski*, 2003]. A big advantage of the ^{86}Sr-labeling technique compared to the chemical dye techniques is that Sr is a natural component in the skeleton, naturally incorporated into the aragonite skeleton of corals.

[13] Finally, a key observation from the experiment is that the ^{86}Sr label is not continuously distributed along the growth front. Instead, the label forms distinct and often clearly isolated 'hotspots' (Figures 1g, 1h, and 1i). This has at least one important implication of relevance to the conceptual framework of existing geochemical models that seek to explain compositional 'vital' effects in the skeleton. These geochemical models are based on a fluid reservoir, close in composition to seawater, which is hypothesized to exist between the surface of the forming skeleton and the calicoblastic cell-layer. From this hypothetical reservoir, often referred to as the Extracellular Calcifying Fluid (ECF), the skeleton is believed to form as a result of super-saturation of the fluid that results in physiochemical carbonate precipitation [*Adkins et al.*, 2003; *Gaetani and Cohen*, 2006; *McConnaughey*, 2003]. However, in the incarnation of these models, the ECF reservoir would predict continuous labeling along large stretches of the growth front. This is not observed (Figures 1g and 1i). Therefore, in the case of *Porites porites*, the lateral dimension of the hypothetical ECF reservoir cannot be larger than that of the labeled ^{86}Sr hotspots (i.e., 5–10 μm) and is most certainly not a spatially continuous compartment along the growing surface of the skeleton. Furthermore, recent observations of the interface between the calicoblastic cell-layer and the surface of the growing skeleton suggest that in fact the hypothetical continuous ECF reservoir does not exist, that previously observed sub-skeletal space most likely was an artifact of coral tissue fixation, and that indeed the calicoblastic cells generally are in direct contact with the surface of the growing skeleton, with the exception of a few discrete nanometer scale sub-spaces [*Clode and Marshall*, 2002; *Goldberg*, 2001; *Tambutté et al.*, 2007]. We therefore propose that the heterogeneous distribution of ^{86}Sr label along the growth front is the direct image of spatially heterogeneous cellular activity in the calicoblastic cell-layer, where certain domains or compartments are actively forming skeleton while neighboring cells are inactive. An important challenge in future experiments will be to image the corresponding calicoblastic cell-layer with the NanoSIMS in order to establish if the distribution of the isotopic label in the cell-layer [*Marshall et al.*, 2007] reflects the distribution observed in the skeleton.

[14] **Acknowledgments.** R. Rodolfo-Metalpa and Claude Bouchon are thanked for the collection of the *Porites* colonies and help in the setting up the experiment. N. Benbalagh is thanked for assistance with SEM imaging. This work was funded partly by the Muséum National d'Histoire Naturelle, by the Agence National de la Recherche, by a Lavoisier Fellowship from the French Ministry of Foreign Affairs to FH, and the Polish Ministry of Science and Higher Education, project N307-015733 to

JS. Nicky Allison, Ted McConnaughey and an anonymous reviewer are thanked for constructive criticism, which helped improve the manuscript.

[15] The International Atomic Energy Agency is grateful for the support provided to its Marine Environment Laboratory by the Government of the Principality of Monaco. The National Ion MicroProbe Facility at the Museum National d'Histoire Naturelle was established by funds from the INSU-CNRS, Région Île de France, Ministère délégué à l'Enseignement Supérieur et de la Recherche, and the Muséum itself.

References

Adkins, J. F., et al. (2003), Stable isotopes in deep-sea corals and a new mechanism for "vital effects", *Geochim. Cosmochim. Acta*, *67*, 1129–1143.

Allison, N. (1996), Comparative determination of trace and minor elements in coral aragonite by ion microprobe analysis, with implications from Phuket, southern Thailand, *Geochim. Cosmochim. Acta*, *60*, 3457–3470.

Allison, N., and A. A. Finch (2007), High temporal resolution Mg/Ca and Ba/Ca records in modern *Porites lobata* corals, *Geochem. Geophys. Geosyst.*, *8*, Q05001, doi:10.1029/2006GC001477.

Blamart, D., C. Rollion-Bard, A. Meibom, J.-P. Cuif, A. Juillet-Leclerc, and Y. Dauphin (2007), Correlation of boron isotopic composition with ultrastructure in the deep-sea coral *Lophelia pertusa*: Implications for biomineralization and paleo-pH, *Geochem. Geophys. Geosyst.*, *8*, Q12001, doi:10.1029/2007GC001686.

Chiu, V., and D. H. Haynes (1977), High and low affinity Ca^{2+} binding to the sarcoplasmic reticulum: Use of a high-affinity flourescent calcium indicator, *Biophys. J.*, *8*, 3–22.

Clode, P. L., and A. T. Marshall (2002), Low temperature FESEM of the calcifying interface of a scleractinian coral, *Tissue Cell*, *34*, 187–198.

Cohen, A. L., G. D. Layne, S. R. Hart, and P. S. Lobel (2001), Kinetic control of skeletal Sr/Ca in a symbiotic coral: Implications for the paleotemperature proxy, *Paleoceanography*, *16*, 20–26.

Cole, J. E., et al. (2000), Tropical pacific forcing of decadal SST variability in the western Indian Ocean over the past two centuries, *Science*, *287*, 617–619.

Cuif, J.-P., and Y. Dauphin (1998), Microstructural and physio-chemical characterization of 'centers of calcification' in septa of some Recent scleractinian corals, *Palaontol. Z.*, *72*, 257–270.

Cuif, J.-P., and Y. Dauphin (2005), The environmental recording unit in coral skeletons—A synthesis of structural and chemical evidences for a biochemically driven, stepping-growth process in fibres, *Biogeosciences*, *2*, 61–73.

Cuif, J.-P., et al. (2003), XANES mapping of organic sulfate in three scleractinian coral skeletons, *Geochim. Cosmochim. Acta*, *67*, 75–83.

Dodge, R. E., et al. (1984), Coral calcification rates by the buoyant weight technique: Effects of alizarin staining, *J. Exp. Mar. Biol. Ecol.*, *75*, 217–232.

Fairbanks, R. G., and M. N. Evans (1997), Evaluating climate indices and their geochemical proxies measured in corals, *Coral Reefs*, *16*, S93–S100.

Ferrier-Pagès, C., et al. (2002), Kinetics of strontium uptake in the scleractinian coral *Stylophora pistillata*, *Mar. Ecol. Prog. Ser.*, *245*, 93–100.

Fietzke, J., and A. Eisenhauer (2006), Determination of temperature-dependent stable strontium isotope ($^{88}Sr/^{86}Sr$) fractionation via bracketing standard MC-ICP-MS, *Geochem. Geophys. Geosyst.*, *7*, Q08009, doi:10.1029/2006GC001243.

Gaetani, G. A., and A. L. Cohen (2006), Element partitioning during precipitation of aragonite from seawater: A framework for understanding paleoproxies, *Geochim. Cosmochim. Acta*, *70*, 4617–4634.

Goldberg, W. M. (2001), Desmocytes in the calicoblastic epithelium of the stony coral *Mycetophyllia reesi* and their attachment to the skeleton, *Tissue Cell*, *33*, 388–394.

Huston, M. (1985), Variation in coral growth rates with depth at Discovery Bay, Jamaica, *Coral Reefs*, *4*, 19–25.

Marshall, A. T., et al. (2007), Electron and ion microprobe analysis of calcium distribution and transport in coral tissues, *J. Exp. Biol.*, *210*, 2453–5463.

Marubini, F. (1996), The physiological response of hermatypic corals to nutrient enrichment, Ph.D. thesis, 192 pp., Univ. of Glasgow, Glasgow, U. K.

McConnaughey, T. A. (2003), Sub-equilibrium oxygen-18 and carbon-13 levels in biological carbonates and kinetic models, *Coral Reefs*, *22*, 316–327.

McCulloch, M. T., et al. (1999), Coral record of equatorial sea-surface temperatures during the penultimate deglaciation at Huan Peninsula, *Science*, *283*, 202–204.

Meibom, A., M. Stage, J. Wooden, B. R. Constantz, R. B. Dunbar, A. Owen, N. Grumet, C. R. Bacon, and C. P. Chamberlain (2003), Monthly Strontium/Calcium oscillations in symbiotic coral aragonite: Biological effects limiting the precision of the paleotemperature proxy, *Geophys. Res. Lett.*, *30*(7), 1418, doi:10.1029/2002GL016864.

Meibom, A., J.-P. Cuif, F. Hillion, B. R. Constantz, A. Juillet-Leclerc, Y. Dauphin, T. Watanabe, and R. B. Dunbar (2004), Distribution of magnesium in coral skeleton, *Geophys. Res. Lett.*, *31*, L23306, doi:10.1029/2004GL021313.

Meibom, A., et al. (2006), Vital effects in coral skeletal composition display strict three-dimensional control, *Geophys. Res. Lett.*, *33*, L11608, doi:10.1029/2006GL025968.

Meibom, A., S. Mostefaoui, J.-P. Cuif, Y. Dauphin, F. Houlbrèque, R. Dunbar, and B. Constantz (2007), Biological forcing controls the chemistry of reef-building coral skeleton, *Geophys. Res. Lett.*, *34*, L02601, doi:10.1029/2006GL028657.

Meibom, A., et al. (2008), Chemical variations at ultra-structural length-scales in coral skeleton, *Geochim. Cosmochim. Acta*, *72*, 1555–1569.

Nothdurft, L. D., and G. E. Webb (2007), Microstructure of common reef-building coral genera *Acropora, Pocillopora, Goniastrea* and *Porites*: Constraints on spatial resolution in geochemical sampling, *Facies*, *53*, 1–26.

Reynaud-Vaganay, S., et al. (1999), A novel culture technique for scleractinian corals: Application to investigate changes in skeletal $\delta^{18}O$ as a function of temperature, *Mar. Ecol. Prog. Ser.*, *180*, 121–130.

Rollion-Bard, C., et al. (2003a), Microanalysis of C and O isotopes of azooxanthellate and zooxanthellate corals by ion microprobe, *Coral Reefs*, *22*, 405–415.

Rollion-Bard, C., et al. (2003b), pH control on oxygen isotopic composition of symbiotic corals, *Earth Planet. Sci. Lett.*, *215*, 275–288.

Shirai, K., et al. (2005), Deep-sea coral geochemistry: Implication for the vital effect, *Chem. Geol.*, *224*, 212–222.

Sinclair, D. J. (2005), Correlated trace element "vital effects" in tropical corals: A new geochemical tool for probing biomineralization, *Geochim. Cosmochim. Acta*, *69*, 3265–3284.

Sinclair, D. J., B. Williams, and M. Risk (2006), A biological origin for climate signals in corals—Trace element "vital effects" are ubiquitous in Scleractinian coral skeletons, *Geophys. Res. Lett.*, *33*, L17707, doi:10.1029/2006GL027183.

Stolarski, J. (2003), Three-dimensional micro- and nanostructural charateristics of the scleractinian coral skeleton: A biocalcification proxy, *Acta Palaeontol. Pol.*, *48*, 497–530.

Tambutté, E., et al. (2007), Observations of the tissue-skeleton interface in the scleractinian coral *Stylophora pistillata*, *Coral Reefs*, *26*, 517–529.

Thébault, J., et al. (2006), Evidence of a 2-day periodicity of stria formation in the tropical Comtopallium radula using calcien marking, *Mar. Biol.*, *149*, 257–267.

Veron, J. E. N. (2000), *Corals of the World*, Australian Inst. of Mar. Sci., Townsville, Queensl., Australia.

J.-P. Cuif, UMR8148, IDES, Université Paris XI, F-91405 Orsay CEDEX, France.

I. Domart-Coulon, Département Milieux et Peuplements Aquatiques, UMR5178, Muséum National d'Histoire Naturelle, 55 rue Buffon, F-75005 Paris CEDEX, France.

R. B. Dunbar and F. Houlbrèque, Geological and Environmental Sciences, Stanford University, Stanford, CA 94305-2115, USA.

C. Ferrier-Pagès, Centre Scientifique de Monaco, Avenue Saint Martin, MC-98000 Principality of Monaco, Monaco.

Y. Marrocchi and A. Meibom, Laboratoire de Minéralogie et Cosmochimie du Muséum (LMCM), UMS NanoAnalyses 2679, Muséum National D'Histoire Naturelle, 61 rue Buffon, F-75005 Paris CEDEX, France. (meibom@mnhn.fr)

J. Stolarski, Instytut Paleobiologii PAN, ul. Twarda 51/55, PL-00-818 Warszawa, Poland.